View metadata, citation and similar papers at core.ac.uk

brought to you by CORE

provided by The University of Utah: J. Willard Marriott Digital Library

PHYSICAL REVIEW B VOLUME 49, NUMBER 18 1 MAY 1994-II

First-principles study of crystalline silica

Feng Liu and Stephen H. Garofalini
Department of Ceramics, Rutgers University, Piscataway, New Jeresey 08855-0909

Dominic King-Smith* and David Vanderbilt
Department of Physics and Astronomy, Rutgers University, Piscataway, New Jersey 08855-0849

(Received 8 December 1993)

We have investigated the structural properties of five different crystalline forms of SiO_2 using a first-principles approach. An ultrasoft Vanderbilt pseudopotential is generated for oxygen which enables us to use a small plane-wave cutoff of 25 Ry. The relative stability, the equation of state, and pressure-dependent structural parameters of all five polymorphs have been calculated and found to be in very good agreement with available experimental results.

I. INTRODUCTION

The complex structure and the presence of oxygen atoms conspire to make a first-principles theoretical study of SiO_2 especially difficult. Recently, with the help of newly developed fast iterative algorithms for solving the one-electron Schrödinger equation, several structural forms of crystalline SiO_2 have been successfully studied using pseudopotential density-functional plane-wave methods.[1–3] However, the use of conventional norm-conserving oxygen pseudopotentials[4,5] in these studies requires a relatively large plane-wave cutoff, rendering this approach problematic for more studies on complex systems involving defects, surfaces, and disorder. A more efficient approach has recently been developed which combines the use of an ultrasoft separable pseudopotential by Vanderbilt[6] with a Car-Parrinello (CP) -type algorithm.[7] This method has successfully been applied to study applications as diverse as phase transitions of ice under high pressure,[8] the structure of liquid copper,[9] and ferroelectricity in barium titanate.[10] In this paper we present an application of this method to study five different structural forms of SiO_2 (α,β-quartz, α,β-cristobalite, and stishovite). An ultrasoft pseudopotential has been generated for oxygen to correctly predict the energetics and the structural properties for all five forms of silica with a plane-wave cutoff of only 25 Ry.

SiO_2 has been one of the most extensively studied materials due to its application potential in ceramic and glass industries as well as in optical fibers, microelectronics, and catalysis. On the other hand, it is also one of the most difficult materials to study. The first difficulty arises from its structural complexity. Silica can assume many different structural forms.[11,12] Among them the most common ones are quartz, cristobalite, coesite, and stishovite. The common prominent feature in most of these structures are corner-sharing tetrahedral units of silicon with four nearest-neighbor oxygen atoms. One exception is stishovite in which silicon is sixfold coordinated with oxygens arranged in a distorted octahedron. These structures also have subtle differences in energy since they differ from each other mainly in the way in which the tetrahedral units are connected. The second difficulty is due to the presence of oxygen atoms. It is well known that the first row nonmetal elements (e.g., oxygen) and the first row transition-metal elements are problematic species in the conventional norm-conserving pseudopotential scheme. Due to the lack of corresponding core states for cancellation, the tightly bound $2p$ or $3d$ valence wave functions of these elements are sharply peaked. As a result, a relatively hard pseudopotential has to be generated to describe them and a relatively large number of plane-wave basis functions are required in solid-state calculations. Because of these difficulties only a few crystalline structures of SiO_2 have been investigated with first-principles techniques, although the complex bonding situation in silica with a mixture of ionic and covalent interactions speaks to the necessity for a treatment on an *ab initio* microscopic level.

The motivation of the present work is to apply one of the most efficient first-principles techniques to date to systematically study the various systems of crystalline SiO_2. Of the five systems we study, we note that certain aspects of most structures have previously been studied by *ab initio* pseudopotential methods. For example, Allan and Teter[1] determined the structural parameters at ambient conditions for α-quartz, α-cristobalite, and stishovite. Chelikowsky and co-workers[2,3] investigated the structural properties and their pressure dependence for α-quartz and stishovite. Also, we have recently demonstrated a plausible structural model for β-cristobalite.[13] In the present study, we carried out an extensive study to calculate the ground-state energetics and structural parameters at ambient conditions for all five systems. We also calculated the equations of state and the pressure dependence of structural parameters for three low-temperature phases (α-quartz, α-cristobalite, and stishovite). We believe the current work will be of interest for several reasons. First, we treat a larger range of silica structures than has been treated in any previous theory. The fact that we use a uniform theoretical treatment facilitates systematic comparisons and identifications of trends between these five crystal structures. Second, no previous theory on the *ab initio* level has appeared for structural determination of β-quartz.

0163-1829/94/49(18)/12528(7)/$06.00

©1994 The American Physical Society

Third, we give some additional details of our calculation on β-cristobalite which did not appear in our previous published paper.[13] Finally, we demonstrate that the use of ultrasoft pseudopotentials makes it possible to obtain accurate results, in good agreement with experiment and previous theories, using a plane-wave cutoff of only 25 Ry. Since the best that has previously been achieved with norm-conserving oxygen pseudopotentials is 40 Ry,[1] the present method shows great promise of future applications.

The article is organized as follows. In Sec. II, we will give a brief review of the theoretical method and the generation of silicon and oxygen pseudopotentials. The results are presented and discussed in Sec. III. Section IV presents a summary and conclusion.

II. THEORETICAL METHOD

Our computational method can be described as a combination of the ultrasoft pseudopotential scheme[6] with the preconditioned conjugate gradient algorithm.[14–15] Most previous *ab initio* studies on silica have been done with the conventional norm-conserving pseudopotential scheme. As shown by Hamann, Schlüter, and Chiang,[4] the merit of this scheme is that the norm-conserving condition ensures that the energy derivative of the all-electron (AE) and pseudo-wave-function logarithmic derivatives are identical at the construction energy so that the pseudoatom can correctly reflect the scattering properties of the AE atom in the energy range of valence electrons. On the other hand, in the case of a nodeless oxygen $2p$ valence wave function the pseudo-wave-function has to be restricted to satisfy the norm-conserving condition, which results in a hard pseudopotential. Many attempts have been made to improve the softness and smoothness of the conventional norm-conserving pseudopotentials,[5,16,17] but the norm-conserving condition still imposes a severe limit on the improvement.

An ultrasoft pseudopotential scheme has recently been introduced by Vanderbilt.[6] In this scheme, the correct scattering properties are obtained by matching the energy derivative of pseudo-wave-function logarithmic derivative to the AE one at the construction energy without imposing the norm-conservation constraint. Thus, much more flexibility is allowed, and the pseudo wave function can be made as smooth as possible, leading to an "ultrasoft" potential. In practice, we have adopted a variant of the optimization scheme of Rappe *et al.*[17] to construct a pseudo wave function that converges at a target plane-wave cutoff. Due to the relaxation of norm conservation, a localized core-region charge augmentation function $Q_{ij}(r)$ is introduced.[18] As a result, the dual condition ($E_c^{\rm dens}=4E_c^{\rm wf}$) between the energy cutoff of charge density ($E_c^{\rm dens}$) and wave function ($E_c^{\rm wf}$) is no longer guaranteed, since the augmentation function usually requires higher cutoff. The pseudization of $Q_{ij}(r)$ will reduce the charge cutoff $E_c^{\rm dens}$, but, in some cases,[9] a separate high cutoff is still needed. In many other cases, such as for silicon and oxygen as studied here, the dual condition can be restored by optimally pseudizing $Q_{ij}(r)$. We have used an optimization scheme similar to that used by Rappe *et al.*[17] for the wave function combined with the refinement of use of L-dependent cutoff $r_{\rm inner}$.[18] Besides the ultrasoftness, the Vanderbilt pseudopotential also has the advantage of better transferability. The scattering properties are correctly reflected over a wide energy range because the AE and pseudoatom logarithmic derivatives are matched by construction at more than one energy for each angular momentum channel. This ingredient also makes it possible to choose valence states with different principle quantum numbers, n, but same angular momentum quantum number, l, which is incompatible with the conventional schemes.[19]

We have used neutral $2s^22p^4$ as the reference state to construct the oxygen potential. Both s and p channels were treated as nonlocal components for the pseudopotential and two construction energies (s and p eigenvalues) were used for each channel to improve the transferability. As discussed in the case of the oxygen dimer,[6] the convergence of the pseudopotential can be improved by increasing the cutoff radius r_c. However, for r_c too large, the transferability may suffer when the interatomic spacing is small. Also, increasing r_c may increase the hardness of the charge augmentation function $Q_{ij}(r)$ which would invalidate the dual condition ($E_c^{\rm dens}=4E_c^{\rm wf}$) when r_c is too large. In the silica system the nearest-neighbor distance between Si and O is about 3.0 a.u. We used a cutoff radius r_c of 1.3 a.u. for both s and p valence wave functions and 1.0 a.u. for the local potential. The L dependent $r_{\rm inner}$ for pseudizing $Q_{ij}(r)$ are 0.7, 0.8, and 0.9 a.u. for $L=0$, 1, and 2, respectively.

The silicon pseudopotential was generated from the ionized $3s^23p^1$ reference configuration. Nonlocal projectors in s and p channels were introduced with one construction energy for each channel. The cutoff radius for both s and p valence functions and for the local potential were taken to be 1.4 and 1.0 a.u., respectively. The cutoff $r_{\rm inner}$ was chosen to be 0.8 ($L=0$), 0.9 ($L=1$), and 1.0 a.u. ($L=2$). This potential gives rise to a lattice constant of 10.16 a.u. for bulk diamond silicon which is about 0.9% too small when compared to the experimental value.

In the solid-state calculation of all five structures, the total-energy and force calculations have been carried out within the local density approximation (LDA). The Ceperley-Alder[20] form of the exchange correlation potential was adopted. The electronic solution was obtained via a preconditioned conjugate gradient minimization scheme[14,15] and the optimal structural parameters for each structure were determined. We have found that a plane-wave cutoff of 20 Ry is sufficient for the convergence of lattice constants and internal coordinates of all structures, but we opted to use a larger cutoff of 25 Ry to ensure the accuracy in energetics for comparing the small energy differences among the different structures and in the elastic properties. The total energy changes by less than 0.003 eV/atom on increasing the cutoff from 25 to 40 Ry in all structures. Detailed information on unit cell, crystal symmetry, and k-point sampling for each individual structure will be given in the next section. We have tried to use equivalent k-point sampling as much as possi-

ble for different structures to make parallel comparison in energies, in addition to making sure of the k-point sampling convergence. In most cases, k-point sampling has converged at about 0.002 eV/atom on going to the next higher k-point set.

III. RESULTS AND DISCUSSIONS

A. Energetics and equation of state

We have calculated the binding energy of each structure as a function of atomic volume. At a given volume, the optimal lattice parameters and internal atomic coordinates are determined based on minimization of the total energy using calculated forces. The binding energy was obtained in reference to isolated atom energies including the spin-polarization corrections. A Murnaghan equation of state was then fit to a few calculated points to determine the equilibrium volume, the cohesive energy, the bulk modulus (B_0), and the pressure derivative of the bulk modulus (B_0'). In Fig. 1 we show the binding energy of α-quartz, β-quartz, α-cristobalite, β-cristobalite, ideal β-cristobalite, and stishovite, as a function of volume. The resultant cohesive energies are presented in Table I in comparison with experimental results which were obtained by adding the formation enthalpy of the low temperature (α) phases at room temperature or the high temperature (β) phases at the appropriate transition temperatures[21,22] with the cohesive energy of bulk silicon and the dissociation energy of the oxygen dimer.[23] It is well known that LDA normally overestimates the cohesive energy. Our calculated cohesive energies for all five structures are consistently higher than the experimental ones by about 15–20%. The relative stability of different phases is correctly predicted and α-quartz is the most stable structure. As we expected, the error in energy differences is much smaller than that in absolute energies. The calculated energy differences between α-quartz and α-cristobalite (0.03 eV/molecular unit) and between β-quartz and β-cristobalite (0.0 eV/molecular unit) agree perfectly with experiment, while the calculated energy differences between α-phase and β-phase for both quartz and cristobalite are slightly smaller than the experimental data. We believe the agreement would be slightly improved with the inclusion of the temperature effect missing in the calculation. However, the calculated energy difference between α-quartz and stishovite of 0.07 eV per molecular unit is a few times lower than the experimental value, although it agrees well with the previous first-principles calculation[3] of 0.1 eV per molecular unit. The reason for this discrepancy is not completely clear. We note that stishovite has a totally different structural topology from the other four tetrahedral-network structures. In general, the energy differences among different phases are very small. This is understandable for α-,β-quartz and α-,β-cristobalite, since all these structures are composed of SiO_4 tetrahedral units that are connected in slightly different ways. But it is a little bit surprising for stishovite, which has a totally different structural topology. One would also expect that[3] the stability of quartz and cristobalite over stishovite will be further enhanced at finite temperature due to the larger entropy contribution from the more open structures.[3]

From the Murnaghan fit of binding energy curves in Fig. 1, we have constructed the equations of state. In Fig. 2 we plot the calculated volume vs pressure curve for

TABLE I. Cohesive energies (eV/molecular unit). Q=quartz; C=cristobalite.

Structure	Theory	Experiment[a]
α-Q	22.42	19.23
β-Q	22.38	19.18
α-C	22.39	19.20
β-C	22.38	19.18
stishovite	22.35	18.71

[a]References 21–23.

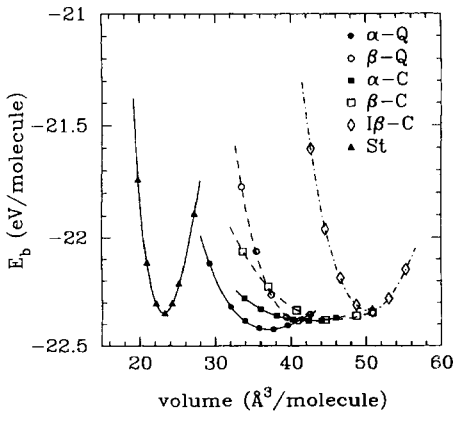

FIG. 1. Binding energies as a function of volume for α-,β-quartz (Q), α-β-cristobalite (C), ideal (I) β-cristobalite (C), and stishovite (St). The symbols are calculated data points and the lines are Murnaghan fits to the calculated points.

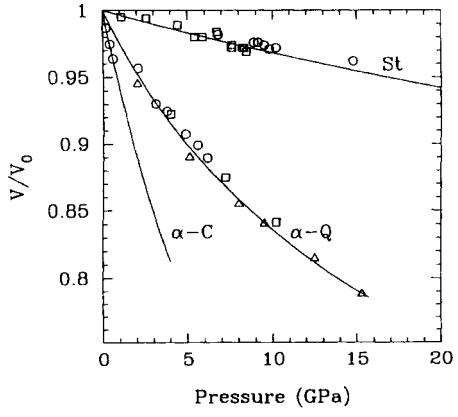

FIG. 2. Equations of state (curves) for α-quartz (Q), α-cristobalite (C), and stishovite (St) derived from Murnaghan fits as in Fig. 1. The volume has been normalized to ambient volume (V_0). The symbols are experimental data from Refs. 25 (circle), 26 (square), and 27 (triangle) for α quartz, Ref. 33 for α-cristobalite, and Refs. 37 (circle) and 38 (square) for stishovite.

α-quartz, α-cristobalite, and stishovite in comparison with available experimental data. The agreement is fairly good. From the slope of the curve, we can see that α-cristobalite is most compressible, indicating a most open structure. In contrast, stishovite is most closely packed.

B. Structural parameters and their pressure dependence

The optimal lattice parameters and internal atomic coordinates of each structure were determined based on total energy and forces calculations at a few selected volumes. The final set of structural parameters at the equilibrium volume shown in Tables II–VI is based on an interpolation of all the calculated points. Also shown in the tables are the bulk modulus (B_0), and the derivative of bulk modulus (B_0'), obtained from the Murnaghan fit. Our calculated results are compared with selected experimental results which are considered to be the most recent and reliable ones and with some previous first-principles calculations.

1. α-quartz

α-quartz has a hexagonal $P3_221$ space-group symmetry. The primitive unit cell contains 9 atoms. At a given volume, six parameters have to be determined to specify the structure, namely, lattice parameters a and c (or c/a), and internal parameters (u,x,y,z). We will use (u,v,w) to denote internal coordinates for silicon and (x,y,z) for oxygen throughout. The calculation was conducted at three special k points[24] $(\frac{2}{9},0,\frac{1}{4})$, $(\frac{4}{9},0,\frac{1}{4})$, and $(\frac{5}{9},\frac{1}{3},\frac{1}{4})$. The results are presented in Table II. The volume (or pressure) dependence of lattice constants and internal parameters is plotted in Figs. 3 and 4, respectively. The crystal structure of α-quartz at room temperature and ambient pressure has been studied many times experimentally.[25] In Table II we have chosen the recent refinement by Levien, Prewitt, and Weidner[25] for our comparison. The dependence of the structural properties on pressure has also been studied by several different experimental groups[25–27] which were included in Figs. 3 and 4. The agreement between present theory and experiments is excellent for both structural parameters and their pressure dependence. Lattice constants a and c (see Fig. 3) decrease monotonically as volume decreases (or pressure increases) with a slightly faster change in a, indicating a small increase in c/a ratio. All internal atomic coordinates (see Fig. 4) change almost linearly with increasing pressure. Note that we also included in Figs. 3 and 4 a recent pseudopotential calculation by Chelikowsky *et al.*[2] The general agreement between the two theories is very good, except that their calculated value of c is a little bit larger at ambient pressure, and decreases slightly faster with increasing pressure.

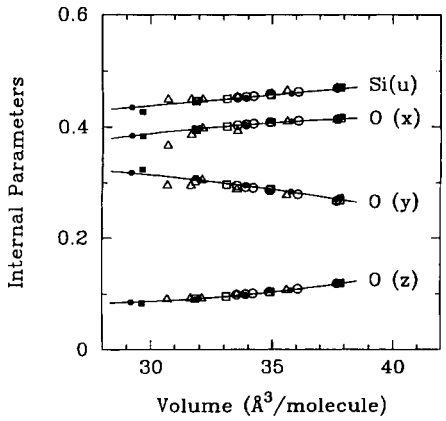

FIG. 3. Lattice constant as a function of volume for α-quartz. Solid dots are calculated points and lines are polynomial fits to the calculated points as a guide to the eye. Circles, squares, and triangles are experimental data from Refs. 25, 26, and 27, respectively. Solid squares are pseudopotential calculations from Ref. 2.

2. β-quartz

β-quartz is believed to have an overall hexagonal $P6_222$ space-group symmetry, but whether atoms are actually located at the high symmetrical positions or dynamically jump between two lower-symmetry (α-quartz) twin configurations leading to an averaged high symmetry is

TABLE II. Structural parameters of α-quartz ($P3_221$).

Parameter	Experiment	This work	Error (%)	Other theory
a (Å)	4.9160[a]	4.8756	−0.82	4.9134[b]
c (Å)	5.4054[a]	5.4052	−0.004	5.4052[b]
Si (u)	0.4697[a]	0.4654	−0.92	0.4638[b]
O (x)	0.4135[a]	0.4125	−0.24	0.4081[b]
O (y)	0.2669[a]	0.2745	2.84	0.2758[b]
O (z)	0.1191[a]	0.1143	−4.03	0.1215[b]
B_0 (Mbar)	~0.34–0.37[c]	0.37		0.38[d]
B_0'	~5–6[c]	4.3		3.9[d]

[a]Reference 25.
[b]Reference 1.
[c]References 25–27.
[d]Reference 2.

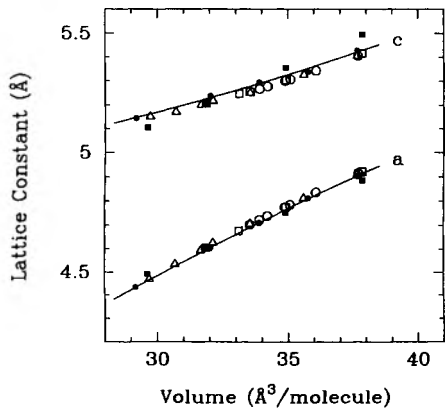

FIG. 4. Internal parameters as a function of volume for α-quartz. Notation is the same as in Fig. 3.

TABLE III. Structural parameters of β-quartz ($P6_222$).

Parameter	Experiment[a]	This work	Error (%)
a (Å)	4.9977	5.0526	1.10
c (Å)	5.4601	5.5488	1.62
O (x)	0.4144	0.4178	0.82

[a]Reference 30.

still a controversial subject.[28,29] In our calculation, we have constrained nine atoms in the unit cell into the hexagonal $P6_222$ space group. The k-point sampling of the calculation is chosen to be the same as for α-quartz. Three parameters ($a,c,x=2y$) have been determined to specify the structure which is shown in Table III. Also included in the table are the experimental results by Wright and Lehmann.[30] The fact that the calculated cohesive energy (see Table I) as well as structural parameters for β-quartz agree very well with experiments indicates the plausibility of a structure with well-defined atom positions, although we cannot rule out the dynamic picture based on our calculation. A more thorough first-principles calculation is needed to further resolve the problem.

3. α-cristobalite

The structure of α-cristobalite is well established with a tetragonal $P4_12_11$ space-group symmetry. The primitive unit cell contains twelve atoms. At a given volume, six parameters have to be determined to specify the structure, namely, lattice parameters a and c (or c/a), and internal parameters (u,x,y,z). The calculation was conducted at two special k points[31] ($\frac{1}{4},0,\frac{1}{4}$), and ($\frac{1}{4},\frac{1}{2},\frac{1}{4}$). The results are presented in Table IV. The pressure (or volume) dependence of lattice constant and internal parameters is plotted in Figs. 5 and 6, respectively. Unlike α-quartz, little experimental information on α-cristobalite is available. Pluth and Smith[32] have determined its crystal structure from time-of-flight neutron-powder-diffraction data at low temperature up to 10 K (see Table IV). The pressure dependence of the structure has been very recently studied by Parise *et al.*[33] up 1.2 GPa. At 1.2 GPa they observed a phase transition to a lower symmetry phase. Our calculation agrees very well with their results as shown in Figs. 5 and 6 for the change of structural parameters and in Table IV for the bulk modulus. Both lattice constants a and c (see Fig. 5) decrease monotonically with increasing pressure. But unlike α-quartz, the c lattice constant changes faster than a, resulting in a decrease in c/a ratio on going to high pressure. All internal atomic coordinates (see Fig. 5) change almost linearly with increasing pressure.

TABLE IV. Structural parameters of α-cristobalite ($P4_12_12$).

Parameter	Experiment	This work	Error (%)	Other theory
a (Å)	4.9570[a]	4.9586	0.03	4.9590[b]
c (Å)	6.8903[a]	6.9074	0.25	6.9060[b]
Si (u)	0.3047[a]	0.3028	−0.62	0.3030[b]
O (x)	0.2381[a]	0.2383	0.08	0.2380[b]
O (y)	0.1109[a]	0.1093	−1.44	0.1112[b]
O (z)	0.1826[a]	0.1816	−0.55	0.1825[b]
B_0 (Mbar)	0.150[c]	0.148	−1.33	
B_0'		2.41		

[a]Reference 32.
[b]Reference 1.
[c]Reference 33.

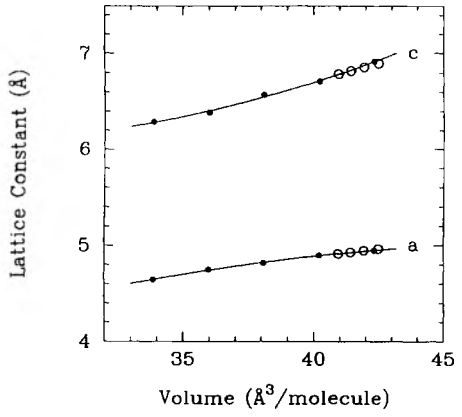

FIG. 5. Lattice constant as a function of volume for α-cristobalite. Solid dots are calculated points and lines are polynomial fits to the calculated points as a guide to the eye. Circles are experimental data from Ref. 33.

4. β-cristobalite

The determination of the structure for β-cristobalite has a long and controversial history. It has an overall $Fd3m$ symmetry and involves orientational disorder. Recently, we have demonstrated the plausibility of a structure for β-cristobalite consisting of domains of $I42d$ symmetry, and provided strong evidence against other proposed models, based on first-principles total energy and

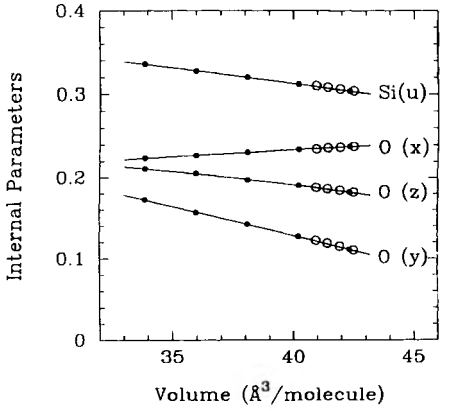

FIG. 6. Internal parameters as a function of volume for α-cristobalite. Notation is the same as in Fig. 5.

TABLE V. Structural parameters of β-cristobalite ($F4d2$).

Parameter	Experiment[a]	This work	Error (%)
a (Å)	7.131	7.147	0.22
c (Å)	0.125	(in $Fd3m$ position)	
O (x)	0.079	0.081	2.53

[a]Reference 34.

lattice dynamics calculations. The details of the study can be found in Ref. 13. In the present study, we have repeated part of the calculations using a primitive tetragonal cell containing twelve atoms constrainted to $I42d$ symmetry. Two special k points were used, as for α-cristobalite. The original calculation was conducted with a larger conventional cubic cell with 24 atoms in $F4d2$ symmetry. Virtually identical structural parameters have been obtained which are shown in Table V, together with a comparison with experimental results of Wright and Leadbetter.[34]

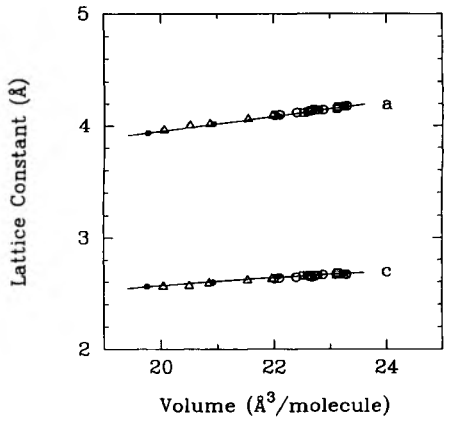

FIG. 7. Lattice constant as a function of volume for stishovite. Solid dots are calculated points and lines are polynomial fits to the calculated points as a guide to the eye. Circles, squares, and triangles are experimental data from Refs. 37, 38, and 39, respectively.

5. *Stishovite*

In Table VI we present the structural parameters for stishovite. Stishovite belongs to space group $P4_2/mnm$. There are six atoms in the tetragonal unit cell with three independent parameters (a,c,x) at a given volume. Six special k points[35] have been used in the calculation: $(\frac{3}{8},\frac{7}{8},\frac{7}{8})$, $(\frac{7}{8},\frac{7}{8},\frac{3}{8})$, $(\frac{3}{8},\frac{3}{8},\frac{3}{8})$, $(\frac{7}{8},\frac{7}{8},\frac{7}{8})$, $(\frac{7}{8},\frac{3}{8},\frac{3}{8})$, and $(\frac{3}{8},\frac{3}{8},\frac{7}{8})$. Similar to the case of α-quartz, there is a vast quantity of experimental results available for stishovite.[3] For the comparison of structural parameters in Table VI, we have chosen recent x-ray single crystal and powder-diffraction experiments of Spackman, Hill, and Gibbs.[36] In Fig. 7 we plot the calculated lattice constants a and c as a function of volume (pressure). The experimental results presented in Fig. 7 are from Liu, Bassett, and Takahashi,[37] Bassett and Barnett,[38] and Tsuchida and Yagi.[39] We found that lattice constants a and c decrease almost linearly with increasing pressure with a slight increase in c/a ratio similar to α-quartz.

From Tables II–VI and Figs. 3–7, we can see that the calculated structural parameters and their pressure dependence for all studied structures agree very well with available experimental results and other first-principles studies. The errors are generally within 2%. The agreement for the bulk modulus and its pressure derivatives is also reasonably good but less accurate. Part of the error is due to the fact that these quantities are found to be more sensitive to the Murnaghan fit to the calculated data.

TABLE VI. Structural parameters of stishovite ($P4_2/mnm$).

Parameter	Experimental	This work	Error (%)	Other theory
a (Å)	4.1773[a]	4.1612	−0.39	4.2550[b]
c (Å)	2.6655[a]	2.6671	0.06	2.6040[b]
O (x)	0.30614[a]	0.30552	−0.20	0.3082[b]
B_0 (Mbar)	~3.06–3.13[c]	2.82		2.92[d]
B_0'	~1.7–6.0[c]	5.60		5.86[d]

[a]Reference 36.
[b]Reference 1.
[c]References 37–39.
[d]Reference 3.

IV. CONCLUSION

In summary, we have carried out an extensive study of the energetics and the structural properties of five crystalline forms of silica based on first-principles total energy and force calculations. The relative stability of different phases has been correctly predicted, with decreasing stability from quartz to cristobalite and from cristobalite to stishovite. The energy differences between different structures have been found to be very small (less than 0.05 eV per molecular unit in most cases) as one would expect from the small differences in structural topology. The calculated structural parameters at ambient conditions agree very well with experiments. Also, the calculated equations of state and the pressure dependence of structural parameters are in good agreement with experiments. We found that the c/a ratio increases with increasing pressure for both α-quartz and stishovite but decreases for α-cristobalite.

The ultrasoft pseudopotential scheme allowed us to achieve the same degree of accuracy as previous pseudopotential theories but with a much smaller plane-wave cutoff (25 Ry vs 40 Ry), and the preconditioned conjugate gradient algorithm increased the convergence rate of the calculation considerably over the usual steepest decent algorithm (about 10 times for the current problem). We believe that the combination of these two techniques makes our approach uniquely suited for efficient first-principles calculations on complex systems like silica. This is partly demonstrated by the fact that all the calculations done

here have been carried out on an IBM RISC/6000 workstation. We think the present study provides reason for optimism regarding the possibility of future investigations on more complex systems involving defects, surfaces, and disorder.

ACKNOWLEDGMENTS

This work was partially supported by U.S. DOE-OBES Grant No. DE-FG05-88ER45368 and partially by U.S. NSF Grant No. DMR-8907553.

*Present address: Biosym Technologies, Inc., San Diego, CA 92121.

[1]D. C. Allan and M. P. Teter, Phys. Rev. Lett. **59**, 1136 (1987); J. Am. Ceram. Soc. **73**, 3274 (1990).

[2]J. R. Chelikowsky, H. E. King, Jr., N. Troullier, J. L. Martins, and J. Glinnemann, Phys. Rev. Lett. **65**, 3309 (1990); J. R. Chelikowsky, N. Troullier, J. L. Martins, and H. E. King, Jr., Phys. Rev. B **44**, 489 (1991).

[3]N. R. Keskar, N. Troullier, J. L. Martins, and J. R. Chelikowsky, Phys. Rev. B **44**, 4081 (1991).

[4]D. R. Hamann, M. Schlüter, and C. Chiang, Phys. Rev. Lett. **43**, 1494 (1979); G. B. Bachelet, D. R. Hamann, and M. Schlüter, Phys. Rev. B **26**, 4199 (1982).

[5]N. Troullier and J. L. Martins, Solid State Commun. **74**, 613 (1990); Phys. Rev. B **43**, 1993 (1991); **43**, 8861 (1991).

[6]David Vanderbilt, Phys. Rev. B **41**, 7892 (1990).

[7]K. Laasonen, R. Car, C. Lee, and D. Vanderbilt, Phys. Rev. B **43**, 6796 (1991).

[8]C. Lee, D. Vanderbilt, K. Laasonen, R. Car, and M. Parrinello, Phys. Rev. Lett. **69**, 462 (1992); Phys. Rev. B **47**, 4863 (1993).

[9]A. Pasquarello, K. Laasonen, R. Car, C. Lee, and D. Vanderbilt, Phys. Rev. Lett. **69**, 1982 (1992).

[10]R. D. King-Smith and D. Vanderbilt, Ferroelectrics **136**, 85 (1992).

[11]R. W. G. Wyckoff, *Crystal Structures*, 2nd ed. (Interscience, New York, 1965).

[12]R. B. Sosman, *The Phase of Silica* (Rutgers University Press, New Brunswick, NJ, 1965).

[13]F. Liu, S. H. Garofalini, R. D. King-Smith, and D. Vanderbilt, Phys. Rev. Lett. **70**, 2750 (1993).

[14]R. D. King-Smith and D. Vanderbilt, Phys. Rev. B **49**, 5828 (1994).

[15]M. P. Teter, M. C. Payne, and D. C. Allan, Phys. Rev. B **40**, 12 255 (1989).

[16]D. Vanderbilt, Phys. Rev. B **32**, 8412 (1985).

[17]A. M. Rappe, K. M. Rabe, E. Kaxiras, and J. D. Joannopoulos, Phys. Rev. B **41**, 1227 (1990).

[18]K. Laasonen, A. Pasquarello, R. Car, C. Lee, and D. Vanderbilt, Phys. Rev. B **47**, 10 142 (1993).

[19]F. Liu, S. H. Garofalini, R. D. King-Smith, and D. Vanderbilt, Chem. Phys. Lett. **215**, 401 (1993).

[20]D. M. Ceperley and B. J. Alder, Phys. Rev. Lett. **45**, 566 (1980); D. Ceperley, Phys. Rev. B **18**, 3126 (1978).

[21]P. Richet, Y. Bottinga, L. Denielou, J. P. Petitet, and C. Tequi, Geochim. Cosmochim. Acta **46**, 2639 (1982).

[22]J. L. Holm, O. J. Kleppa, and E. F. Westrum, Jr., Geochim. Cosmochim. Acta **31**, 2289 (1967).

[23]*CRC Handbook of Chemistry and Physics*, 64th ed. (CRC, Boca Raton, FL, 1983).

[24]D. J. Chadi and M. L. Cohen, Phys. Rev. B **8**, 5747 (1973).

[25]L. Levien, C. T. Prewitt, and D. J. Weidner, Am. Mineralog. **65**, 920 (1980).

[26]J. Glinnemann, H. E. King, Jr., H. Schulz, Th. Hahn, S. J. La Placa, and F. Dacol, Z. Kris. **198**, 177 (1992).

[27]R. M. Hazen, L. W. Finger, R. J. Hemley, and H. K. Mao, Solid State Commun. **72**, 507 (1989).

[28]S. Tsuneyuki, H. Aoki, and M. Tsukada, Phys. Rev. Lett. **64**, 776 (1990).

[29]Y. Tezuka, S. Shin, and M. Ishigame, Phys. Rev. Lett. **66**, 2356 (1991).

[30]A. F. Wright and M. S. Lehmann, J. Solid State Chem. **36**, 371 (1981).

[31]B. A. Evarestov and V. P. Smirnov, Phys. Status Solidi B **119**, 9 (1983).

[32]J. J. Pluth and V. Smith, J. Appl. Phys. **57**, 1045 (1985).

[33]J. B. Parise, D. J. Weidner, A. Yeganeh-Haeri, J. D. Jorgensen, and M. A. Saltzberg (unpublished).

[34]A. F. Wright and A. J. Leadbetter, Philos. Mag. **31**, 1391 (1975).

[35]P. J. Lin-Chung, Phys. Status Solidi B **85**, 743 (1978).

[36]M. A. Spackman, R. J. Hill, and G. V. Gibbs, Phys. Chem. Minerals **14**, 139 (1987).

[37]L. G. Liu, W. A. Bassett, and T. Takahashi, J. Geophys. Res. **79**, 1160 (1974).

[38]W. A. Bassett and J. D. Barnett, Phys. Earth Planet. Interiors **3**, 54 (1970).

[39]Y. Tsuchida and T. Yagi, Nature (London) **340**, 217 (1989).